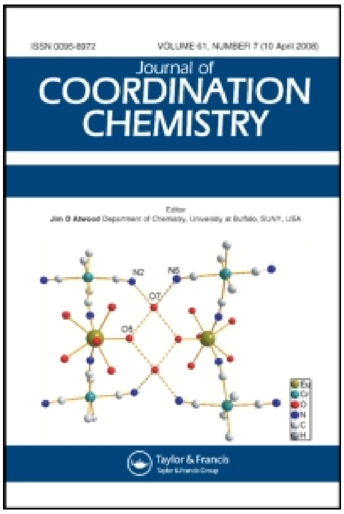

Journal of Coordination Chemistry
Publication details, including instructions for authors and subscription information:
http://www.informaworld.com/smpp/title~content=t713455674

Syntheses and structures of mononuclear and binuclear transition metal complexes (Cu, Zn, Ni) with (salicylideneglycine and imidazole)

Yong Heng Xing[a]; Jing Han[a]; Guang Hua Zhou[a]; Zheng Sun[b]; Xing Jing Zhang[a]; Bao Li Zhang[a]; Yuan Hong Zhang[a]; Hou Qun Yuan[a]; Mao Fa Ge[b]
[a] Bioinorganic Laboratory, College of Chemistry and Chemical Engineering, Liaoning Normal University, Dalian, P.R. China [b] Institute of Chemistry, The Chinese Academy of Sciences, Beijing, P.R. China

First published on: 20 July 2007

To cite this Article Xing, Yong Heng , Han, Jing , Zhou, Guang Hua , Sun, Zheng , Zhang, Xing Jing , Zhang, Bao Li , Zhang, Yuan Hong , Yuan, Hou Qun and Ge, Mao Fa(2008) 'Syntheses and structures of mononuclear and binuclear transition metal complexes (Cu, Zn, Ni) with (salicylideneglycine and imidazole)', Journal of Coordination Chemistry, 61: 5, 715 — 730, First published on: 20 July 2007 (iFirst)

To link to this Article: DOI: 10.1080/00958970701389989

URL: http://dx.doi.org/10.1080/00958970701389989

Journal of Coordination Chemistry
Vol. 61, No. 5, 10 March 2008, 715–730

Taylor & Francis
Taylor & Francis Group

Syntheses and structures of mononuclear and binuclear transition metal complexes (Cu, Zn, Ni) with (salicylideneglycine and imidazole)

YONG HENG XING*†, JING HAN†, GUANG HUA ZHOU†,
ZHENG SUN‡, XING JING ZHANG†, BAO LI ZHANG†,
YUAN HONG ZHANG†, HOU QUN YUAN† and MAO FA GE‡

†Bioinorganic Laboratory, College of Chemistry and Chemical Engineering, Liaoning Normal University, Dalian 116029, P.R. China
‡Institute of Chemistry, The Chinese Academy of Sciences, Beijing 100080, P.R. China

(*Received 13 December 2006; in final form 26 January 2007*)

Four transition metal (Cu(II), Zn(II) and Ni(II)) complexes with a Schiff-base ligand (salicylideneglycine) have been synthesized. All complexes have been characterized by elemental analysis, IR spectra and UV-vis spectroscopy. Single-crystal analyses were performed with $(C_9H_7NO_3)Cu(C_3H_4N_2)$ (**1**), $(C_9H_7NO_3)Zn(C_3H_4N_2)_2$ (**2**), $(C_9H_7NO_3)_2Ni_2(C_3H_4N_2)_4$ (**3**) and $(C_9H_7NO_3)Ni(C_3H_4N_2)_2(C_4H_5N_2O)\cdot CH_3OH\cdot 0.5H_2O$ (**4**) and fluorescence spectra and thermogravimetric analyses were also carried out. Structural analyses show that **1**, **2** and **4** have similar coordinated modes with the tridentate amino-Schiff-base ligand, but differ from the binuclear nickel complex **3**. The tridentate amino-Schiff-base ligand contains aliphatic nitrogen, phenoxy, and carboxylic oxygen as three donor atoms. In addition, inter- and intra-molecular hydrogen bonds are also discussed.

Keywords: Transition metal complexes; Salicylideneglycine ligand; Supramolecular assembly; Hydrogen bond; Crystal structures

1. Introduction

Schiff-base ligands coordinate to many metals in various oxidation states and have attracted much attention [1]. By modifying the structures of Schiff bases, many well-designed Schiff-base ligands have been prepared, for instance, macrocycle Schiff base [2, 3], pyridine-containing dicarbonyl ligands [4], chiral Schiff bases [5–7], and so on. Large numbers of researchers have indicated that complexes with Schiff-base ligands have biological activity. For example, in the 1960s, Popp *et al.* studied several Schiff bases of benzaldehyde N mustards and found them active enough in an experiment tumor system to merit clinical trials [8]. Study of antibacterial and antitumor activity of Schiff-base compounds and their metal complexes are still widely discussed. Different Schiff-base ligands and metals show different character enticing

---

*Corresponding author. Email: yhxing2000@yahoo.com

Journal of Coordination Chemistry
ISSN 0095-8972 print/ISSN 1029-0389 online
DOI: 10.1080/00958970701389989

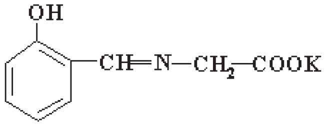

Figure 1. The structure of potassium salt of salicylideneglycine.

synthesis of new Schiff-base metal complexes in different ways [9, 10], such as [M(L)(bipy-amine)(H_2O)] or [M(L)(bendan)(H_2O)], where M = Mn(II), Co(II), Ni(II), Cu(II), Zn(II) and Cd(II) (KHL = potassium salt of salicylideneglycine and bipyramine = 2,2′-bipyridylamine and bendandi(benzylidene)-1,8-diaminonaphthalene) [11–16]. The structure of the amino-Schiff-base ligand is shown in figure 1. Properties and preparations have been reported, but no crystal structures. In this article we report the syntheses, crystal structures and properties of four new transition metal complexes with an amino-Schiff-base (salicylideneglycine) ligand: $(C_9H_7NO_3)Cu(C_3H_4N_2)$ (**1**), $(C_9H_7NO_3)Zn(C_3H_4N_2)_2$ (**2**), $(C_9H_7NO_3)_2Ni_2(C_3H_4N_2)_4$ (**3**) and $(C_9H_7NO_3)Ni(C_3H_4N_2)_2(C_4H_5N_2O) \cdot CH_3OH \cdot 0.5H_2O$ (**4**).

2. Experimental section

2.1. *Instruments and reagents*

Elemental analyses were performed on a PE 240C automatic analyzer. The IR spectra were determined by a JASCO FT/IR-480 PLUS Fourier Transform spectrometer (200–4000 cm^{-1}, with pressed KBr pellets); UV-vis spectra were determined by a JASCO V-570 UV-vis spectrometer (200–1100 nm, CH_3OH solution); fluorescence spectra were determined by JASCO FP-6500 spectrofluorimeters (CH_3OH solution). All chemicals used were of analytical grade and used without further purification. The amino-Schiff-base ligand was prepared by modified literature method [16] and all other reactants were used as purchased. The reactions were carried out at room temperature.

2.2. *Preparation of HL*

2.2.1. Potassium salt of salicylideneglycine (KHL) [16]. A solution of potassium hydroxide (10 mmol, 0.56 g) in 30 mL absolute alcohol was added to glycine (10 mmol, 0.75 g). The mixture was stirred until a clear solution appeared. Then the ethanolic solution (100 mL) of salicylaldehyde (10 mmol, 1.22 g) was added dropwise. Precipitation occurred by diffusion of excess absolute diethyl ether into the solution. The orange product was filtered and dried in a vacuum desiccator. Yield: 1.59 g (63%). Anal. Calcd for $C_9H_8NO_3K$: C, 49.77; H, 3.69; N, 5.45%. Found: C, 48.98; H, 3.58; N, 5.33%; m.p. 207°C.

2.2.2. Preparation of 3-methyl-5-pyrazolone ($C_4H_6N_2O$) [17]. To a three-necked round-bottom flask equipped with a condenser to which was attached a drying tube, a thermometer and an addition funnel was added a solution of 15.60 g (0.12 mol) ethyl acetoacetate and absolute ethanol. Then 6.25 g (0.10 mol) of hydrazine hydrate (80%) was added and the temperature was kept at 50°C. Upon completion of the addition, the reaction mixture was refluxed for 3 h, cooled, and the precipitate was filtered off, washed with methanol and ethanol and then recrystallized from ethanol to get the white target product. Yield: 88.7%. Anal. Calcd for $C_4H_6N_2O$: C, 48.98; H, 6.12; N, 28.57%. Found: C, 48.58; H, 6.01; N, 27.98%; m.p. 221.6°C.

2.3. *Preparation of complexes*

2.3.1. Preparation of $(C_9H_7NO_3)Cu(C_3H_4N_2)$ (1) and $(C_9H_7NO_3)Zn(C_3H_4N_2)_2$ (2). A methanol solution of KHL 1.0 mmol (0.22 g), 1.0 mmol (0.07 g) of imidazole ($C_3H_4N_2$) and 1.0 mmol (0.20 g) of $Cu(CH_3COO)_2 \cdot H_2O$ was stirred for 3 h. The colour of the solution changed from blue to cyan and a precipitate formed which was filtered off, washed with methanol and ethanol extensively, then dried under vacuum to afford 0.20 g of the product, with the yield being 64.8% (based on $Cu(CH_3COO)_2 \cdot H_2O$). Anal. Calcd for $C_{12}H_{11}N_3O_3Cu$: C, 46.64; H, 3.56; N, 13.60%. Found: C, 46.58; H, 3.51; N, 13.63%. IR (KBr, ν cm^{-1}): 3446s, 3136w, 2926w, 2852w, 1642s, 1578s, 1536m, 1453m, 1383s, 1293m, 1150m, 1071m, 761s, 657m, 535m, 481w, 417w. UV-vis (λ_{max}/nm, ε_{max} mol^{-1} cm^2): 222 (3.66×10^5), 240 (3.59×10^5), 268 (2.08×10^5), 368 (8.77×10^5).

The preparation of **2** is almost the same as that of **1**, but having 1 : 1 : 2 metal-ligand mole ratio of $Zn(CH_3COO)_2 \cdot 2H_2O$, KHL and imidazole ($C_3H_4N_2$). About 0.29 g of the product was obtained with the yield being 76.8% (based on $Zn(CH_3COO)_2 \cdot 2H_2O$). Anal. Calcd for $C_{15}H_{14}N_5O_3$ Zn: C, 47.66; H, 3.71; N, 18.53%. Found: C, 47.61; H, 3.65; N, 18.50%. IR (KBr, ν cm^{-1}): 3421m, 3129m, 3079m, 2932m, 2857m, 2637m, 1638s, 1593s, 1528m, 1470s, 1455m, 1395s, 1353m, 1327m, 1291m, 1187m, 1150s, 1072s, 766s, 659s, 529m, 471w, 458w, 337w. UV-vis (λ_{max}/nm, ε_{max} mol^{-1} cm^2): 240 (1.86×10^5), 270 (1.45×10^5), 362 (1.09×10^5).

2.3.2. Preparation of $(C_9H_7NO_3)_2Ni_2(C_3H_4N_2)_4$ (3). A mixture of $Ni(CH_3COO)_2 \cdot 4H_2O$ (0.5 mmol, 0.12 g), KHL (0.5 mmol, 0.11 g) and imidazole ($C_3H_4N_2$) (1.0 mmol, 0.06 g) was added to 10 mL CH_3OH. The mixture was stirred for 3 h to get a green solution; after about 20 days, there were a few green crystals in the green solution. Yield: 0.26 g, 69.90% based on ($Ni(CH_3COO)_2 \cdot 4H_2O$). Anal. Calcd for $C_{30}H_{30}N_{10}O_6Ni_2$: C, 48.38; H, 4.03; N, 18.82%. Found: C, 48.40; H, 4.09; N, 18.76%. IR (KBr, ν cm^{-1}): 3424m, 3122m, 3067w, 2957w, 1659s, 1597s, 1542m, 1467m, 1446s, 1392s, 1378s, 1320w, 1291s, 1263w, 1147m, 1120m, 1078s, 1067m, 839m, 770s, 519m, 487m, 452w. UV-vis (λ_{max}/nm, ε_{max} mol^{-1} cm^2): 240 (2.35×10^5), 326 (2.95×10^4), 412 (2.01×10^4).

2.3.3. Preparation of $(C_9H_7NO_3)Ni(C_3H_4N_2)_2(C_4H_5N_2O) \cdot CH_3OH \cdot 0.5H_2O$ (4). A mixture of KHL (0.5 mmol, 0.11 g), $C_4H_6N_2O$ (0.5 mmol, 0.05 g) and $Ni(CH_3COO)_2 \cdot 4H_2O$ (0.5 mmol, 0.12 g) in methanol solution was stirred for 1 h to get a yellow-green solution, then imidazole ($C_3H_4N_2$) (1.0 mmol, 0.06 g) was added to the solution and stirred for 3 h. Finally, a green solution was observed.

After about a month, some green crystals were observed in the solution, collected, and then dried in air. Yield: 0.19 g, 73.48% (based on $Ni(CH_3COO)_2 \cdot 4H_2O$). Anal. Calcd for $C_{20}H_{24}N_7O_{5.5}Ni$: C, 46.41; H, 4.64; N, 18.95%. Found: C, 46.45; H, 4.69; N, 18.86%. IR (KBr, ν cm^{-1}): 3401m, 2965w, 1650s, 1597s, 1541m, 1507m, 1470m, 1445s, 1386s, 1280m, 1154m, 1072s, 788m, 760s, 528m, 464w, 417w. UV-vis (λ_{max}/nm, ε_{max} mol^{-1} cm^2): 238 (1.21×10^4), 336 (3.97×10^3), 410 (4.52×10^3).

2.4. *X-ray data collection and refinement of crystal structures*

Crystals of **1**–**4** were mounted on a glass fiber for X-ray measurement. Reflection data were collected at room temperature on an APEX II CCD diffractometer with graphite-monochromated Mo-Kα radiation ($\lambda = 0.7107$ Å) and $\omega - 2\theta$ scan mode. Intensity data were corrected for Lorentz and polarization effects and absorption (φ scans). The crystal data, data collection, and refinement details are summarized in table 1.

The structures were solved by direct methods using SHELXS-86 and refined using SHELXTL-97. All non-hydrogen atoms were refined anisotropically and hydrogen atoms were included in calculated positions, constrained to ride on their carbon atoms with group U_{iso} values assigned. Atomic scattering factors and anomalous dispersion terms were as in SHELXTL-97. The drawings were made with Diamond and all calculations were performed on a Pentium 4 computer.

3. Results and discussion

3.1. *Synthesis*

The four complexes were synthesized in methanol at room temperature. We also tried to synthesize them by the hydrothermal method in different solvents (mixture solution of water-methanol, water and *N*,*N*-dimethylformamide), but had no better results. Synthetic method of **4** is the same as that of **1**–**3**, the only difference is that 3-methyl-5-pyrazolone was also used as one ligand except for KHL and imidazole ligand. Complex **1** was dark green and very tiny, **2** was yellow, and **3** and **4** were green, but the colour of **4** was deeper than **3**. The complexes were all soluble in methanol, DMF, $CHCl_3$ and CH_2Cl_2, dimethyl sulphoxide, pyridine, CH_3CN and THF, and insoluble in hexane and ether. The reaction process is shown in the scheme 1.

3.2. *Spectroscopic characterization*

3.2.1. IR spectra of complexes. The infrared spectra of **1**–**4** are consistent with the structural data presented in table 2. The strong $\upsilon_{C=N}$ bands for **1** and **2** at 1638 and 1642 were shifted to lower frequency compared to the strong band due to $\upsilon_{C=N}$ at 1645 cm^{-1} in the amino-Schiff base [16, 18], but for **3** and **4** the strong $\upsilon_{C=N}$ bands at 1659 and 1650 cm^{-1} shifted to higher frequency. Two strong and sharp bands of **1**–**4** in the 1578–1597 cm^{-1} and 1383–1395 cm^{-1} region are attributed to asymmetric and symmetric stretching vibrations of the coordinated carboxylates [16, 19]. The spectra

Table 1. Crystallographic data for **1–4**.

Formula	$C_{12}H_{11}CuN_3O_3$	$C_{15}H_{14}N_5O_3Zn$	$C_{30}H_{30}N_{10}Ni_2O_6$	$C_{20}H_{24}N_7NiO_{5.5}$
M (g mol^{-1})	308.78	377.68	744.06	509.17
Crystal system	Monoclinic	Triclinic	Triclinic	Monoclinic
Space group	$P2_1/c$	$P\text{-}\bar{1}$	$P\text{-}\bar{1}$	$P2/c$
a (Å)	11.0601(12)	8.608(4)	9.5281(12)	9.955(8)
b (Å)	11.5163(13	9.683(4)	9.6978(12)	13.922(11)
c (Å)	9.6865(11)	10.836(5)	9.7154(12)	17.300(14)
α (°)	90	88.964(6)	76.882(2)	90
β (°)	103.1880(10)	66.644(6)	79.524(2)	96.402
γ (°)	90	85.468(5)	66.3100(10)	90
V (Å^3)	1201.2(2)	2641.9(6)	796.47(17)	2383(3)
Z	4	2	1	4
D_{Calcd}	1.707	1.517	1.551	1.442
Crystal size (mm^3)	0.08 × 0.12 × 0.20	0.10 × 0.17 × 0.24	0.20 × 0.14 × 0.22	0.20 × 0.22 × 0.18
F(000)	628	1092	384	1076
μ(Mo-Kα) (cm^{-1})	1.825	1.509	1.242	0.864
θ (°)	1.89 to 28.97	2.05 to 25.20	2.16 to 29.02	1.88 to 25.24
Reflections collected	7313	4199	5028	11,465
Independent reflections ($I > 2\sigma(I)$)	2487	2714	3644	2147
Parameters	172	433	433	305
$\Delta(\rho)$ (e Å^{-3})	0.294 and −0.402	0.424 and −0.368	0.500 and −0.327	0.974 and −0.613
Goodness-of-fit	1.055	1.027	1.018	0.974
R^a	0.0275 (0.0346)^b	0.0423 (0.0611)^b	0.0348 (0.0451)^b	0.0612 (0.1530)^b
$wR_2{}^a$	0.0689 (0.0721)^b	0.0933 (0.1046)^b	0.0788 (0.0854)^b	0.1413 (0.1935)^b

[a] $R = \Sigma\|F_o| - |F_c\|/\Sigma|F_o|$; $wR_2 = [\Sigma(w(F_o^2 - F_c^2)^2/[\Sigma(w(F_o^2)^2]^{1/2}$; $[F_o > 4\alpha(F_o)]$; [b] Based on all data.

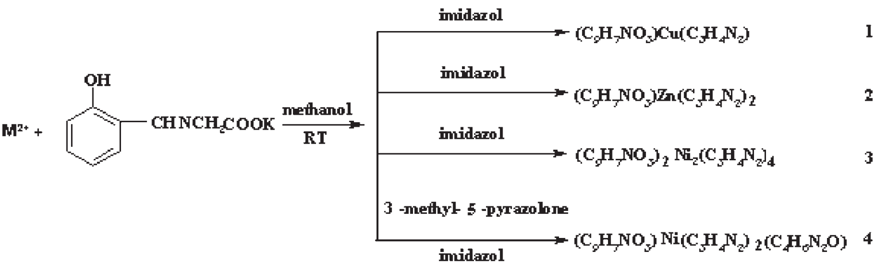

Scheme 1. The synthesis processes of the complexes **1**–**4**.

Table 2. Infrared spectral data of complexes **1**–**4** (cm^{-1}).*

Complexes	**1**	**2**	**3**	**4**
$\upsilon_{(C=C)\,\mathrm{aromatic}}$	1536m	1528m	1542m	1541m
$\upsilon_{(C\text{–}H)\,\mathrm{aromatic}}$	761s	766s	770s	760s
$\upsilon_{(C=N)}$	1642s	1638s	1659s	1650s
$\upsilon_{\mathrm{as}(COO\text{–})}$	1578s	1593s	1597s	1597s
$\upsilon_{\mathrm{s}(COO\text{–})}$	1383s	1395s	1378s	1386s
$\upsilon_{(C\text{–}N)}$	1150m	1150s	1147m	1154m
$\upsilon_{(M\text{–}O)\,\mathrm{aromatic}}$	481w	471w	487m	464w
$\upsilon_{(M\text{–}O)C=O}$	417w	458w	452w	417w
$\upsilon_{(M\text{–}N)}$	535m	529m	519m	528m

*s (strong), m (medium), w (weak).

had bands in the range 1528–1542 cm^{-1} and 760–770 cm^{-1}, which could be assigned to $\upsilon_{(C\text{–}H)\,\mathrm{aromatic}}$ and $\upsilon_{(C=C)\,\mathrm{aromatic}}$ stretching vibration, respectively. For **1** and **2**, the bands at 1150 cm^{-1} are due to C–N stretching; for **3** and **4** the $\upsilon_{(C\text{–}N)}$ bands are at 1147 and 1154 cm^{-1}. Ligand coordination to the metal centre is confirmed by three bands appearing for $\upsilon_{(M\text{–}N)}$ at 519–535 cm^{-1}, $\upsilon_{(M\text{–}O)\,\mathrm{hydroxyl}}$ at 464–487 cm^{-1}, and $\upsilon_{(M\text{–}O)C=O}$ at 417–458 cm^{-1} for **1**–**4** [16].

3.2.2. UV-visible absorption spectroscopy. Electronic absorption spectra of **1**–**4** in CH_3OH have similar absorption patterns. The sharp and strong high-energy absorption bands at 222, 268 and 240 nm for **1**, 270 and 240 nm for **2**, 240 nm for **3** and 238 nm for **4**, are assigned as π–π_2^* transitions of the aromatic-like chromophore from imidazolyl or benzyl. Bands at 368 nm for **1**, 362 nm for **2**, 326 and 412 nm for **3** and 336 and 410 nm for **4** are attributed to the π–π_1^* transitions of the *O*-hydroxy of the amino-Schiff base [20]. Compared to the electronic spectrum of the amino-Schiff base with bands at 218, 258 and 378 nm, the absorption spectra of all complexes are red-shifted, showing amino-Schiff base coordinated to the transition metal atoms.

3.2.3. Fluorescence spectra. The fluorescence emission spectra of the four complexes (**1**–**4**) were taken in MeOH solution under the same conditions. The emission peaks are at 301 and 469 for **1**, 446 for **2**, 300 and 470 for **3**, and 301 and 470 for **4**. Comparing the emission spectral data of free ligand (amino-Schiff base), it is suggested the emission spectra of the complexes originate from π–π^* or amino-Schiff-base ligand to metal

Table 3. Selected bond lengths (Å) and angles (°) for **1**.

Cu(1)–O(1)	1.9214(13)	O(1)–Cu(1)–N(3)	92.63(6)
Cu(1)–N(3)	1.9339(15)	O(1)–Cu(1)–N(1)	90.74(6)
Cu(1)–N(1)	1.9618(15)	N(3)–Cu(1)–N(1)	172.50(7)
Cu(1)–O(2)	1.9944(13)	O(1)–Cu(1)–O(2)	171.53(6)
C(7)–N(3)	1.283(2)	N(3)–Cu(1)–O(2)	83.51(6)
C(9)–O(3)	1.242(2)	N(1)–Cu(1)–O(2)	92.24(6)
C(9)–O(2)	1.269(2)	C(12)–N(1)–Cu(1)	127.30(13)
C(10)–N(1)	1.366(3)	C(10)–N(1)–Cu(1)	113.39(11)
C(11)–N(2)	1.349(3)	C(7)–N(3)–Cu(1)	127.04(12)
C(12)–N(1)	1.312(3)	C(8)–N(3)–Cu(1)	115.17(12)
C(12)–N(2)	1.328(3)	C(1)–O(1)–Cu(1)	128.17(14)
N(3)–C(8)	1.457(2)	C(9)–O(2)–Cu(1)	126.82(14)

charge-transition. Complex **2** exhibits an intense blue emission at 445 nm upon 260 nm excitation, different from the other complexes, showing that luminescence of the complexes is related not only to the configuration of amino-Schiff-base ligand, but also to coordinated metal atoms.

3.3. *Structural description*

The molecular structure of **1**, as determined by X-ray crystallography, reveals a square plane consisting of two nitrogen atoms, two oxygen atoms and a copper atom. The major bond distances and angles are listed in table 3. The copper is coordinated to N1 from imidazolyl, and N3, O1, and O2 from the amino-Schiff-base ligand, as depicted in figure 2(a). Coordination of the amino-Schiff-base ligand is as described [21]. The angles of the O1–Cu1–N3, O1–Cu1–N1, N3–Cu1–O2 and N1–Cu1–O2 are 92.63(6)°, 90.74(6)°, 83.51(6)° and 92.24(6)°, respectively, which all deviate from 90°, indicating that the structure of **1** is distorted. The average distance of the atoms from the square planar is −0.0242(7) Å. The Cu1–O1 length (1.921(1) Å) is shorter than that of the Cu1–O2 (1.994(1) Å). Comparing to other copper complexes, the distance of Cu1–N3 (1.9339(15) Å) is longer than that of Cu–N(1) (1.924(2) Å) in [Cu(bhs)(Hdmpz)] (H_2bhs = *N*-(benzoyl)-*N*′-(salicylidine)hydrazine, Hdmpz = 3,5-dimethylpyrazole) [10], but shorter than that of Cu–N(1) (1.976(3) Å) in the similar copper complex Cu(SAla)Him (SAla = *N*-(2-hydroxybenzyl)-D,L-alanine, Him = imidazole) [9]. The Cu1–N1 (1.9618(15) Å) distance is longer than that of Cu–$N2_{\text{imidazole}}$ (1.947(3), 1.949(2) Å) in two other copper complexes Cu(SAla)Him (SAla = *N*-(2-hydroxybenzyl)-D,L-alanine, Him = imidazole) and Cu(bhs)(Himdz) (H_2bhs = *N*-(benzoyl)-N′-(salicylidine)hydrazine, Himdz = imidazole) [9, 10].

As depicted in figure 2(b), there is a weak interaction (Cu1 ··· O3A, 2.560(1) Å, A: x, $0.5-y$, $-0.5+z$) between O3 and the adjacent copper atom, forming a one-dimensional zigzag chain along the bc plane (figure 2b). The Cu1 ··· O3A distance is obviously longer than that of Cu1–O2 (1.9944(13) Å). The distance between two adjacent copper atoms (Cu1 ··· Cu1A, A: $x, 0.5-y, -0.5+z$) is 6.207(1) Å and the angle of C9A–O3A–Cu1 is 131.31(0)°. In addition, there is a hydrogen bond between O3A (A: $x, 0.5-y, 0.5+z$) from uncoordinated carboxyl oxygen atom of amino-Schiff base and N2B (B: $2-x$, $0.5+y$, $0.5-z$) from the imidazolyl group of an adjacent molecule with a O3A ··· H–N2B distance of 2.755(1) Å as shown in figure 2(c), further extending

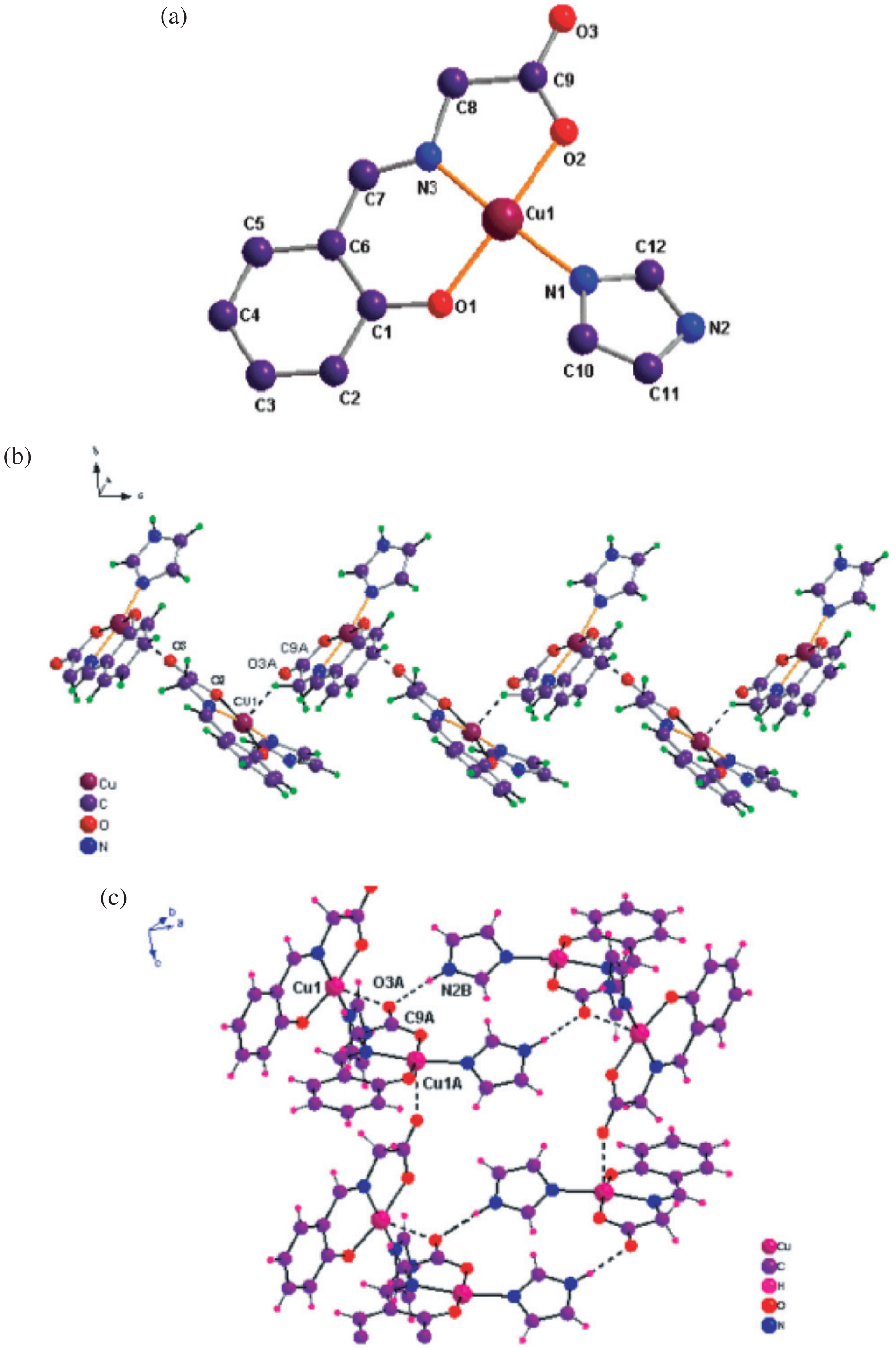

Figure 2. (a) Crystal structure of **1**; (b) A view of the two-dimension sheet formed by a 1,3-*O*,*O*′ bridge; (c) A view of infinite quasi 3-D framework formed through H-bonds in **1**.

to form a three-dimensional porous framework with hydrogen bonds and weak interactions.

The molecular structure of **2** is shown in figure 3(a), featuring the zinc in a five-coordinate anomalistic pyramidal geometry. The O1, O2 and N1 from amino-Schiff-base ligand and N2 from one imidazolyl group occupy the basal plane, while N4 from the other imidazolyl group occupies the apical position. The Zn1 centre lies −0.426(5) Å above the N1–O1–N2–O2 coordination plane. The average deviation

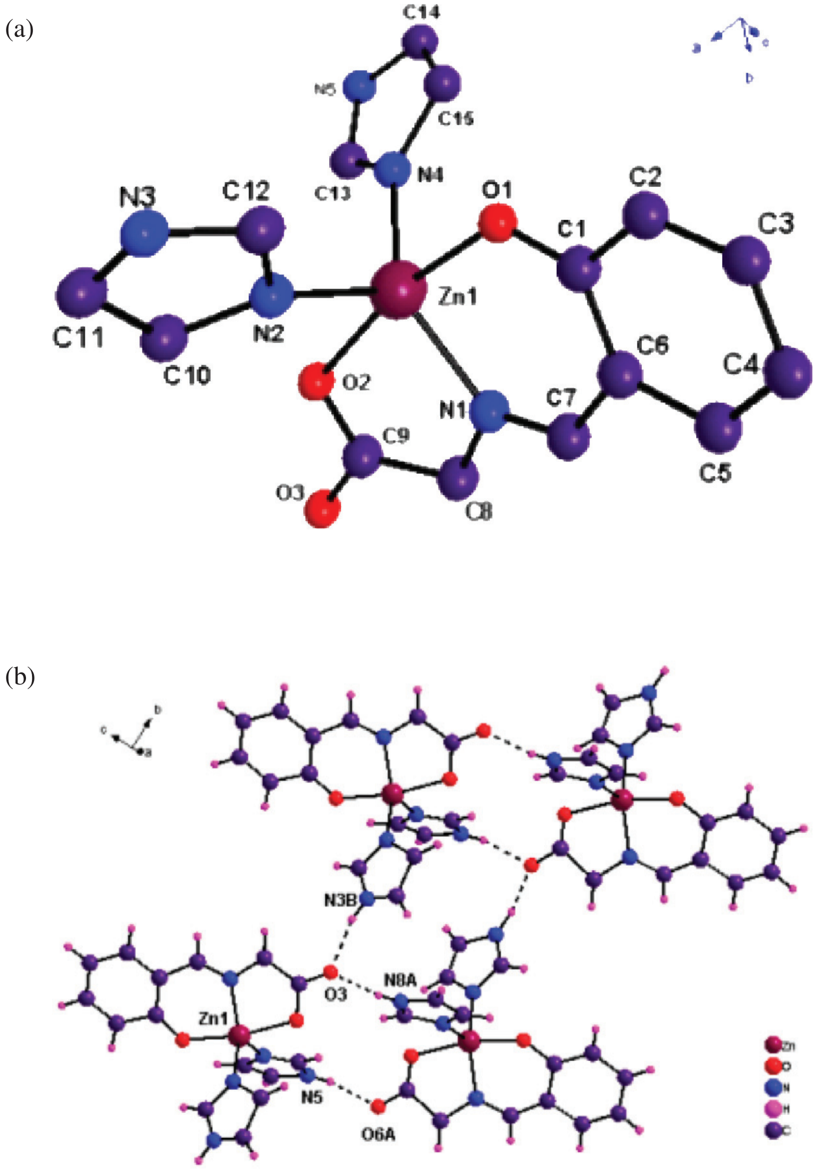

Figure 3. (a) Crystal structure of **2**; (b) A view of infinite quasi 3-D framework formed through H-bonds in **2**.

Table 4. Selected bond lengths (Å) and angles (°) for **2**.

Zn(1)–N(4)	1.975(14)	N(2)–C(12)	1.334(17)	N(4)–Zn(1)–N(2)	106.6(6)	O(1)–Zn(1)–O(2)	168.9(5)
Zn(1)–N(2)	1.981(15)	N(3)–C(11)	1.17(2)	N(4)–Zn(1)–N(1)	129.0(6)	C(1)–O(1)–Zn(1)	124.9(11)
Zn(1)–N(1)	2.034(14)	N(4)–C(13)	1.25(2)	N(2)–Zn(1)–N(1)	123.7(5)	C(9)–O(2)–Zn(1)	113.0(11)
Zn(1)–O(1)	2.036(13)	N(5)–C(13)	1.328(19)	N(4)–Zn(1)–O(1)	94.5(5)	C(7)–N(1)–Zn(1)	125.4(12)
Zn(1)–O(2)	2.201(11)	N(6)–C(22)	1.31(2)	N(2)–Zn(1)–O(1)	92.9(5)	C(8)–N(1)–Zn(1)	116.2(11)
O(1)–C(1)	1.26(2)	N(7)–C(27)	1.31(2)	N(1)–Zn(1)–O(1)	91.1(5)	C(12)–N(2)–Zn(1)	123.7(11)
O(2)–C(9)	1.29(2)	N(8)–C(25)	1.34(2)	N(4)–Zn(1)–O(2)	94.0(5)	C(10)–N(2)–Zn(1)	128.2(11)
O(3)–C(9)	1.259(19)	N(9)–C(30)	1.32(2)	N(2)–Zn(1)–O(2)	91.4(5)	C(13)–N(4)–Zn(1)	128.6(12)
N(1)–C(7)	1.25(2)	N(10)–C(28)	1.25(2)	N(1)–Zn(1)–O(2)	78.0(5)	C(15)–N(4)–Zn(1)	129.2(12)

of the four atoms from the coordination plane is 0.1066(8) Å. The major bond distances and angles are listed in table 4. The Zn1–N1 (amino-Schiff base) distance (2.034(14) Å) is longer than that of the Zn1–N (imidazole) (1.981(15), 1.975(14) Å), but close to that observed in similar complexes [22]. The angles of the N1–Zn1–O1, N1–Zn1–O2, N2–Zn1–O1 and N2–Zn1–O2 are 91.1(5), 78.0(5), 92.9(5) and 91.4(5)°, respectively. One type of hydrogen bond is found in **2** as shown in figure 3(b), hydrogen bonds between an uncoordinated carboxyl oxygen atom and an uncoordinated nitrogen atom from imidazolyl group of a neighboring molecule with distances O3 $\cdots$ H–N8A (2.682(2) Å; A: $1+x, y, -1+z$), O3 $\cdots$ H–N3B (2.805(3) Å; B: $x, 1+y, z$), and N5–H $\cdots$ O6A (2.748(8) Å; A: $1+x, y, -1+z$). Every uncoordinated carboxyl oxygen atom is made a bifurcate hydrogen bond, similarly, extending to form a three-dimensional porous framework.

Figure 4(a) shows the structure of **3**, which is a binuclear nickel complex with two amino-Schiff-base ligands and four imidazole molecules and represents the first example of a binuclear Ni complex with salicylideneglycine. The molecular structure contains two similar mononuclear $Ni(C_3H_4N_2)_2(C_9H_7NO_3)$ units in which the nickel atoms are six coordinate, bonded to three nitrogen atoms from the tridentate amino-Schiff-base ligand and two imidazolyl groups; two Ni atoms are connected by two μ_2-O atoms from the hydroxide groups of two salicylideneglycine ligands. Each nickel in the mononuclear unit is a distorted octahedron, defined by O3, N1 and O1 from an amino-Schiff base, O4 from another amino-Schiff-base ligand and N2 and N4 from two imidazolyl groups. The N4 along with O1, O3 and N1 define the equatorial plane and N2 and O4 occupy the axial positions and form an N2–Ni1–O4 angle of 175.4(4)°, as listed in table 5.

The Ni1 centre lies −0.0470(3) Å below the N1–O1–N4–O3 coordination plane. The deviation of the four atoms (N1, O1, O3, N4) from the equatorial plane is −0.0462(6), 0.0641(5), 0.0615(5) and −0.0325(5) Å, respectively. For Ni2, the N9 atom along with O4, O5 and N6 define the equatorial plane and N7 and O3 occupy the axial positions with N7–Ni2–O3 angle of 176.8(4)°. The Ni2 centre lies 0.0367(3) Å above the N6–O4–N9–O5 coordination plane. The deviation distance of N6, O4, N9 and O5 from the equatorial plane is 0.0435(5), −0.0537(4), 0.0304(4) and −0.0570(5) Å. The Ni1–N_{Schiff} distance (2.008(9) Å) is shorter than the Ni1–$N_{imidazole}$ (2.053(11) Å, 2.098(9) Å) distances; similarly, that of Ni2–$N_{Schiff\ base}$ is also shorter than Ni2–$N_{imidazole}$. The angles of the N1–Ni1–N4, N1–Ni1–O1, N6–Ni2–O4 and N6–Ni2–O5 are 174.6(5), 81.0(4), 87.7(4) and 79.5(4)°, respectively. There is a hydrogen bond in **3** (figure 4b) between an uncoordinated carboxyl oxygen atom and an uncoordinated nitrogen atom from imidazolyl of a neighboring molecule with distances

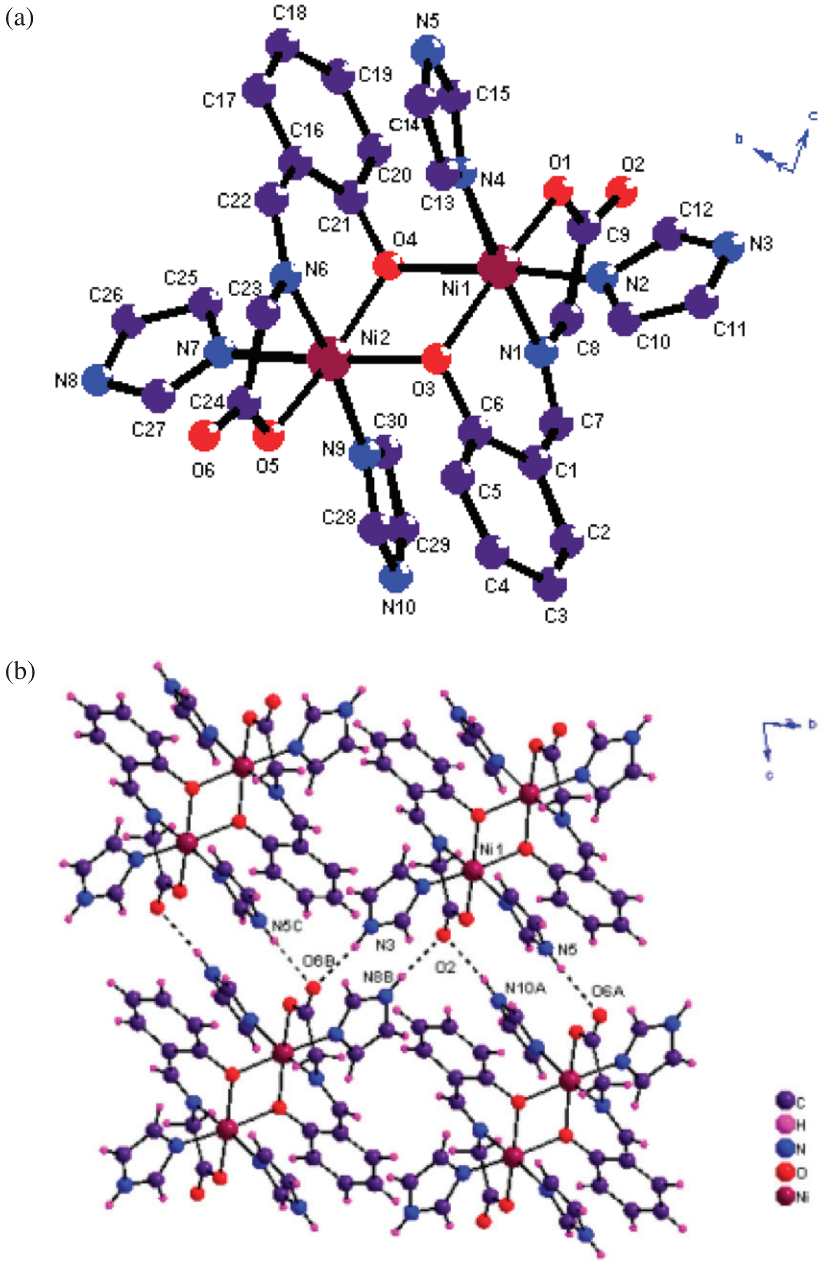

Figure 4. (a) Crystal structure of **3**; (b) A view of infinite quasi 3-D framework formed through H-bonds in **3**.

(O2 $\cdots$ H–N10A, 2.942(17) Å; A: $x, y, 1+z$; O2 $\cdots$ H–N8B, 2.842(14) Å; B: $x, -1+y, 1+z$; N5–H $\cdots$ O6A, 2.945(16) Å; A: $x, y, 1+z$; N3–H $\cdots$ O6B, 2.848(14) Å; B: $x, -1+y, 1+z$) forming a three-dimensional porous framework extended by these intermolecular hydrogen bonds.

Table 5. Selected bond lengths (Å) and angles (°) for **3**.

Ni(1)–N(1)	2.008(9)	N(3)–C(11)	1.291(18)	N(1)–Ni(1)–O(1)	81.0(4)	O(5)–Ni(2)–O(3)	91.3(3)
Ni(1)–N(4)	2.053(11)	N(3)–C(12)	1.309(16)	N(4)–Ni(1)–O(1)	93.6(4)	N(7)–Ni(2)–O(3)	176.8(4)
Ni(1)–O(3)	2.059(9)	N(4)–C(15)	1.331(14)	O(3)–Ni(1)–O(1)	67.1(3)	C(7)–N(1)–Ni(1)	115.1(8)
Ni(1)–N(2)	2.098(9)	N(4)–C(13)	1.369(16)	N(2)–Ni(1)–O(1)	92.0(4)	C(8)–N(1)–Ni(1)	98.3(3)
Ni(1)–O(1)	2.077(9)	C(14)–N(5)	1.401(17)	N(1)–Ni(1)–O(4)	87.0(3)	C(12)–N(2)–Ni(1)	118.1(7)
Ni(1)–O(4)	2.191(7)	N(6)–C(22)	1.329(15)	N(4)–Ni(1)–O(4)	93.1(3)	C(10)–N(2)–Ni(1)	119.9(7)
Ni(2)–N(6)	2.011(10)	N(6)–C(23)	1.466(13)	O(3)–Ni(1)–O(4)	81.2(3)	C(15)–N(4)–Ni(1)	97.9(3)
Ni(2)–O(4)	2.026(8)	N(7)–C(27)	1.276(16)	N(2)–Ni(1)–O(4)	175.4(4)	C(13)–N(4)–Ni(1)	116.8(7)
Ni(2)–N(9)	2.033(10)	N(7)–C(25)	1.361(17)	O(1)–Ni(1)–O(4)	92.1(3)	C(22)–N(6)–Ni(2)	119.3(7)
Ni(2)–O(5)	2.102(9)	C(26)–N(8)	1.406(16)	N(6)–Ni(2)–O(4)	87.7(4)	C(23)–N(6)–Ni(2)	114.0(8)
Ni(2)–N(7)	2.162(8)	N(9)–C(28)	1.296(16)	N(6)–Ni(2)–N(9)	171.7(4)	C(27)–N(7)–Ni(2)	126.8(9)
Ni(2)–O(3)	2.172(8)	N(9)–C(30)	1.357(17)	O(4)–Ni(2)–N(9)	100.6(4)	C(25)–N(7)–Ni(2)	129.2(8)
O(1)–C(9)	1.266(12)	N(10)–C(28)	1.301(16)	N(6)–Ni(2)–O(5)	79.5(4)	C(28)–N(9)–Ni(2)	128.1(9)
O(2)–C(9)	1.255(13)	N(10)–C(29)	1.302(19)	O(4)–Ni(2)–O(5)	166.2(3)	C(30)–N(9)–Ni(2)	122.1(9)
O(3)–C(6)	1.365(13)	N(5)–C(15)	1.360(14)	N(9)–Ni(2)–O(5)	92.2(4)	C(9)–O(1)–Ni(1)	112.9(7)
O(4)–C(21)	1.297(13)	N(8)–C(27)	1.371(14)	N(6)–Ni(2)–N(7)	91.5(4)	C(6)–O(3)–Ni(1)	123.0(8)
O(5)–C(24)	1.235(13)	N(1)–Ni(1)–N(4)	174.6(5)	O(4)–Ni(2)–N(7)	96.5(3)	C(6)–O(3)–Ni(2)	128.3(9)
O(6)–C(24)	1.262(13)	N(1)–Ni(1)–O(3)	87.7(4)	N(9)–Ni(2)–N(7)	87.9(4)	Ni(1)–O(3)–Ni(2)	125.6(9)
N(1)–C(7)	1.231(14)	N(4)–Ni(1)–O(3)	97.7(4)	O(5)–Ni(2)–N(7)	89.1(4)	C(21)–O(4)–Ni(2)	137.3(9)
N(1)–C(8)	1.439(14)	N(1)–Ni(1)–N(2)	91.5(4)	N(6)–Ni(2)–O(3)	85.5(4)	C(21)–O(4)–Ni(1)	123.0(9)
N(2)–C(12)	1.360(17)	N(4)–Ni(1)–N(2)	88.8(4)	O(4)–Ni(2)–O(3)	82.4(3)	Ni(2)–O(4)–Ni(1)	112.8(7)
N(2)–C(10)	1.382(16)	O(3)–Ni(1)–N(2)	94.4(4)	N(9)–Ni(2)–O(3)	95.2(3)	C(24)–O(5)–Ni(2)	127.3(8)

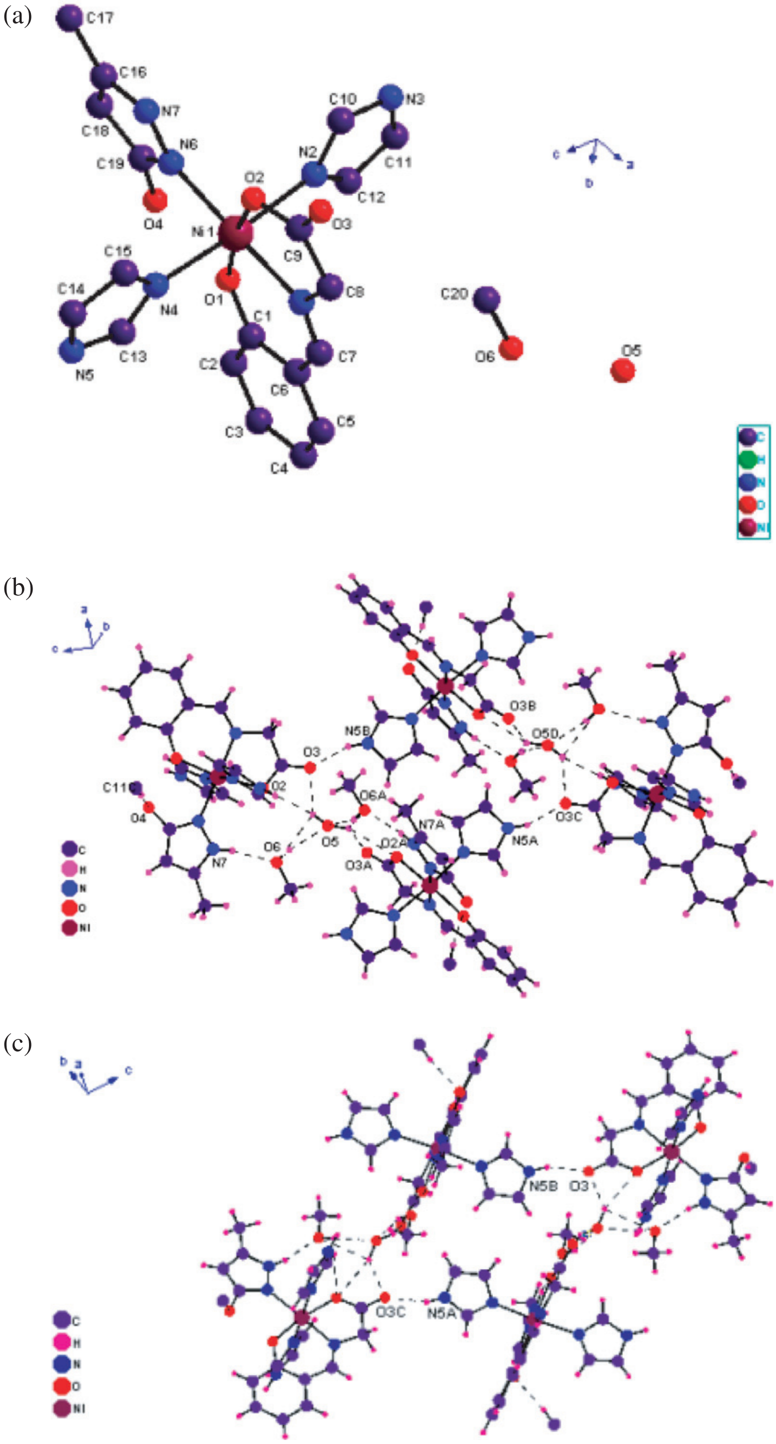

Figure 5. (a) Crystal structure of **4**; (b) A view of infinite quasi 3-D framework formed through H-bonds in **4**; (c) A view of a hydrogen bonding cluster with four units of mononuclear Ni.

Table 6. Selected bond lengths (Å) and angles (°) for **4**.

Ni(1)–O(1)	2.029(5)	N(1)–C(8)	1.458(7)	O(1)–Ni(1)–N(1)	89.1(2)	O(2)–Ni(1)–N(2)	87.53(19)
Ni(1)–N(1)	2.040(5)	N(2)–C(12)	1.286(8)	O(1)–Ni(1)–O(2)	170.70(17)	N(6)–Ni(1)–N(2)	88.66(19)
Ni(1)–O(2)	2.074(4)	N(2)–C(10)	1.389(8)	N(1)–Ni(1)–O(2)	81.66(19)	N(4)–Ni(1)–N(2)	175.1(2)
Ni(1)–N(6)	2.098(5)	N(3)–C(10)	1.334(9)	O(1)–Ni(1)–N(6)	88.4(2)	C(1)–O(1)–Ni(1)	129.6(4)
Ni(1)–N(4)	2.101(5)	N(3)–C(11)	1.359(9)	N(1)–Ni(1)–N(6)	176.4(2)	C(9)–O(2)–Ni(1)	114.1(4)
Ni(1)–N(2)	2.124(5)	N(4)–C(13)	1.307(8)	O(2)–Ni(1)–N(6)	100.92(19)	C(7)–N(1)–Ni(1)	127.4(4)
O(1)–C(1)	1.322(7)	N(4)–C(15)	1.370(8)	O(1)–Ni(1)–N(4)	91.2(2)	C(8)–N(1)–Ni(1)	112.1(4)
O(2)–C(9)	1.270(7)	N(5)–C(13)	1.334(8)	N(1)–Ni(1)–N(4)	93.74(19)	C(12)–N(2)–Ni(1)	127.6(5)
O(3)–C(9)	1.248(7)	N(5)–C(14)	1.343(8)	O(2)–Ni(1)–N(4)	88.82(18)	C(10)–N(2)–Ni(1)	127.9(5)
O(4)–C(19)	1.346(8)	N(6)–C(19)	1.332(7)	N(6)–Ni(1)–N(4)	88.81(19)	C(13)–N(4)–Ni(1)	130.0(5)
O(6)–C(20)	1.333(12)	N(6)–N(7)	1.375(7)	O(1)–Ni(1)–N(2)	92.9(2)	C(15)–N(4)–Ni(1)	125.7(4)
N(1)–C(7)	1.282(8)	N(7)–C(16)	1.339(7)	N(1)–Ni(1)–N(2)	88.98(19)	C(19)–N(6)–Ni(1)	129.7(5)
						N(7)–N(6)–Ni(1)	126.3(4)

The structure of **4**, shown in figure 5(a), is different from **3**. Nickel atom is a distorted octahedron defined by two oxygen atoms and four nitrogen atoms. Nitrogen N6 from the 3-methyl-5-pyrazolone ligand along with O1, O2 and N1 from the amino-Schiff-base ligand define the equatorial plane and the N2 and N4 occupy the axial positions to form an N4–Ni1–N2 angle of 175.1(2)° (table 6). The Ni1 centre lies 0.015(2) Å above the N1–O1–N6–O2 coordination plane. Deviation of N1, O1, N6 and O2 from the equatorial plane is −0.032(2), 0.023(2), −0.028(2) and 0.021(2) Å, respectively. The Ni1–N1 (amino-Schiff base) (2.040(5) Å) is shorter than Ni1–N from the imidazolyl group (2.101(5) Å, 2.124(5) Å) and Ni–N6 from 3-methyl-5-pyrazolone ligand (2.098(5) Å), but longer than the corresponding lengths of the other Ni-Schiff-base complexes [22]. The Ni1–N distances from the imidazolyl group (2.101(5) Å, 2.124(5) Å) are longer than that of Ni–N (imidazolyl, 1.904(5) Å) in another nickel complex (Ni(bhac)(Himdz), H2bhac = acetylacetone benzoylhydrazone, Himdz = imidazole) with a tridentate Schiff base [23]. The angles of the N1–Ni1–O2, O1–Ni1–N1, O1–Ni1–N6 and O2–Ni1–N6 are 81.66(19), 89.1(2), 88.4(2) and 100.92(19)°, respectively. Seven kinds of hydrogen bonds are observed in **4**, as shown in figure 5(b): (i) hydrogen bonds between an uncoordinated nitrogen (donor) from 3-methyl-5-pyrazolone and the oxygen (acceptor) of the lattice methanol with a N7–H ··· O6 distance of 2.849(19) Å; (ii) hydrogen bonds of coordinated carboxyl oxygen (acceptor) from amino-Schiff base with the lattice water (donor) (O2 ··· H–O5: 3.273(24) Å; O5–H ··· O2A: 3.273(24) Å; A: $1-x, y, 1.5-z$); (iii) hydrogen bonds of an uncoordinated carboxyl oxygen (acceptor) from amino-Schiff base with the lattice water (donor) (O3 ··· H–O5: 2.707(12) Å; O5–H ··· O3A: 2.707(12) Å; A: $1-x, y, 1.5-z$); (iv) hydrogen bonds of uncoordinated carboxyl oxygen (acceptor) from amino-Schiff base with the uncoordinated nitrogen (donor) from imidazolyl of an adjacent molecule (O3 ··· H–N5B: 2.741(8) Å; B: $x, 1-y, -0.5+z$); (v) hydrogen bonds of the oxygen (acceptor) of lattice methanol with the lattice water (donor) (O5–H ··· O6: 2.754(14) Å O5–H ··· O6A: 2.754(14) Å; A: $2-x, y, 1.5-z$); (vi) hydrogen bonds of the lattice water (acceptor) with the adjacent oxygen (donor) of the other lattice methanol (O5 ··· H–O6: 2.754(14) Å; O5 ··· H–O6A: 2.754(14) Å; A: $2-x, y, 1.5-z$); (vii) hydrogen bond of carboxyl oxygen (acceptor) from 3-methyl-5-pyrazolone with carbon (donor) from imidazolyl group of the neighboring molecule (O4 ··· H–C11C: 2.894(9) Å). The four mononuclear Ni complexes as a unit are connected by three types of intermolecular hydrogen bonds of O3 ··· H–N5, O5–H ··· O2 and O5–H ··· O3, forming a cluster; the clusters further extend by intermolecular hydrogen bond of O · · · H–C to form a three-dimensional porous framework (figure 5c).

Coordination of the tridentate amino-Schiff base are the same for the complexes, but the torsion angles between the $O_{hydroxyl}$–M–N planes and M–N–$O_{carboxylic}$ (amino-Schiff-base) planes are different: complex **1** (O1–Cu1–N3–O2, 7.57(10)°) > complex **3** (O1–Ni1–N1–O3, 6.09(5)°; O4–Ni2–N6–O5, 5.20(5)°) > complex **2** (O1–Zn1–N1–O2, 2.14(9)°) > complex **4** (O1–Ni1–N1–O2, 0.60(3)°). The M–N (amino-Schiff base) distances for **1**–**4** are different also: complex **1** (1.9339(15) Å) < complex **2** (1.981(15) Å) < complex **3** (2.008(9) Å), (2.011(10) Å) < complex **4** (2.040(5) Å). In amino-Schiff-base ligand, both N–M–O (from hydroxyl) angles in binuclear Ni-Schiff base complex **3** are identical (87.7(4)°), whereas smaller than those of **1** (93.63(6)°), **2** (91.1(5)°) and **4** (89.1(2)°), because in **3** hydroxyl oxygens of amino-Schiff base coordinate to the central metal by double bridges, while the others are terminating coordination modes. The angle of N–M–O (from carboxyl) in **4** (81.66(19)°) is bigger than that of **2** (78.0(5)°), smaller than **1** (83.51(6)°) and close to **3** (81.0(4)°, 79.5(4)°).

3.4. *Thermogravimetric analyses*

The TG-DTG-DTA curves of decomposition of **1** and **2** show one stage of thermal decomposition. The temperature range 179–598 with mass loss of 57.00% for **1** corresponds to loss of amino-Schiff base (calculated value 57.32%). The decomposition of **2** occurs within the temperature range 169–286 with mass loss of 35.93% due to loss of two imidazolyl groups for this thermal event agreeing well with the TG curve (36.01%). The DTA curve of **1** and **2** indicate an endothermic process.

There are two stages of thermal decomposition for **3** in the TG-DTG-DTA curves. The first stage, in the temperature range 221–389, was observed as mass loss of 36.08% corresponding to loss of four imidazolyl groups (calculated value 36.56%). The DTA curve of the complex indicates an endothermic process. The second stage of decomposition occurs within the temperature range 389–724 with mass loss of 15.61% due to the loss of the major part of amino-Schiff-base agreeing with the TG curve (15.72%). The DTA curve of **3** shows that it is an endothermic–exothermic process.

In the TG-DTG-DTA curve of thermal decomposition of **4**, the first stage in the temperature range 200–268 was observed as 19.55% mass loss corresponding to loss of 3-methyl-5-pyrazolone (calculated value 19.05%). The DTA curve of **4** indicates an endothermic process. The second stage in the temperature range 268–682 has mass loss of 34.85% due to loss of amino-Schiff base agreeing with the TG curve (34.76%). The DTA curve of **4** shows that this is also an endothermic-exothermic process.

Thermal decomposition analyses show that although coordination modes of the amino-Schiff base to metal are the same (tridentate), decomposition of **1**, **2**, **3** and **4** are quite different. These reasons originate from steric configuration and ability of different transition metals to coordinate the amino-Schiff base.

Supplementary material

Tables of atomic coordinates, isotropic thermal parameters, and complete bond distances and angles have been deposited with the Cambridge Crystallographic

Data Center. Copies of this information may be obtained free of charge by quoting the publication citation and deposition numbers CCDC: 616657 for **1**, 616658 for **2**, 616656 for **3**, 616655 for **4** from the Director, CCDC, 12 Union Road, Cambridge, CB2 1EZ, UK (Fax: +44-1223-336033; Email: deposit@ccdc.cam.ac.uk; or www: http://www.ccdc.cam.ac.uk).

Acknowledgements

We wish to express our sincere thanks to the National Natural Science Foundation of China (No. 20571036), the Education Foundation of Liaoning Province (No. 05L212), the SRF for ROCS, and SEM for financial assistance.

References

[1] R.H. Holm, G.W. Everett Jr, A. Chakravorty. *Prog. Inorg. Chem.*, **7**, 83 (1966).
[2] S.M. Nelson. *Pure Appl. Chem.*, **52**, 2461 (1980).
[3] J.L. Karn, D.H. Busch. *Nature*, **211**, 160 (1966).
[4] A.M. Herrera, G.V. Kalayda, J.S. Disch, J.P. Wikstrom, I.V. Korendovych, R.J. Staples, C.F. Campana, A.Y. Nazarenko, T.E. Haas, E.V. Rybak-Akimova. *J. C. S. Dalton Trans.*, 4482 (2003).
[5] C. Bolm, F. Bienewald. *Angew. Chem., Int. Ed. Engl.*, **34**, 2640 (1995).
[6] G. Liu, D.A. Cogan, J. Ellman. *J. Am. Chem. Soc.*, **119**, 9913 (1997).
[7] A.H. Velter, A. Berkessel. *Tetrahedron Lett.*, **36**, 1741 (1998).
[8] F.D. Popp, S. Roth, J. Kirby. *J. Med. Chem.*, **6**, 83 (1963).
[9] L.L. Koh, J.O. Ranford, W.T. Robinson, J.O. Svensson, A.L. Chootan, D. Wu. *Inorg. Chem.*, **35**, 6466 (1996).
[10] S. Das, S. Pal. *J. Mol. Struct.*, **753**, 68 (2005).
[11] D.R. Williams. *Chem. Rev.*, **72**, 203 (1972).
[12] N.K. Singh, N. Singh, A. Sodhi, A. Shrivastava, G.C. Prasad. *Transition Met. Chem.*, **21**, 556 (1996).
[13] D.E. Metzler, E.E. Snell. *J. Am. Chem. Soc.*, **74**, 979 (1952).
[14] D.E. Metzler, M. Ikawa, E.E. Snell. *J. Am. Chem. Soc.*, **76**, 648 (1954).
[15] K.M. Patel, K.N. Patel, M.N. Patel. *Synth. React. Inorg. Met.-Org. Chem.*, **30**, 1953 (2000).
[16] P.K. Panchal, M.N. Patel. *Synth. React. Inorg. Met.-Org. Chem.*, **34**, 1277 (2004).
[17] J. De Ruiter, D.A. Cater, W.S. Arledge, P.J. Sullivan. *J. Heterocycl. Chem.*, **24**, 149 (1987).
[18] B.K. Coltrain, S.C. Jackels. *Inorg. Chem.*, **20**, 2032 (1981).
[19] R.V. Singh, J.P. Tandon. *Synth. React. Inorg. Met.-Org. Chem.*, **9**, 121 (1979).
[20] D. Heinert, A.E. Martell. *J. Am. Chem. Soc.*, **85**, 183 (1963).
[21] G. Plesch, C. Frieble, O. Svajleonva, J.K. Smogrovic. *Polyhedron*, **10**, 893 (1991).
[22] L. Wang, X. Zhu, W.-Y. Wong, J.-P. Guo, W.-K. Wong, Z.-Y. Li. *J. C. S. Dalton Trans.*, 3235 (2005).
[23] M. Mukhopadhyay, G. Padmaja, S. Pal, S. Pal. *Inorg. Chem. Commun.*, **6**, 381 (2003).